Intermixing during growth of Cr on Fe(100) studied by proton- and electron-induced Auger-electron spectroscopy

R. Pfandzelter, T. Igel, and H. Winter
Humboldt-Universität zu Berlin, Institut für Physik, Invalidenstrasse 110, 10115 Berlin, Germany
(Received 27 March 1996)

1- and 2-ML Cr films have been grown on Fe(100) under layer-by-layer conditions and studied using Auger electron spectroscopy induced by electrons and grazingly incident protons. Exploiting the different sampling depths for proton and electron excitation, we could quantitatively evaluate the layer-dependent concentration profiles of Cr and Fe near the film surface and their evolution in time. For a coverage of 1 ML, more than half of the deposited Cr atoms have undergone place exchange with Fe substrate atoms, which results in a mixed first and second layer. For 2 ML, the first and second layer consist predominantly of Cr. Long-time measurements show that as-grown 1-ML films are not stable. [S0163-1829(96)11131-0]

Recent studies have shown that epitaxial growth of metal films on metal surfaces involves complex phenomena not anticipated from simple thermodynamic considerations.[1] For a variety of systems the interface between substrate and film is not atomically flat, but intermixing and alloy formation occurs. The atomic scale mechanisms involved include place exchange of condensate and substrate atoms and nucleation and growth of mixed adlayer islands. Continued growth thus may leave many condensate atoms buried in the second and deeper atomic layers. Unprecedented insight into these processes has been obtained from scanning tunneling microscopy (STM),[2,3] where the arrangement of atoms in the topmost atomic layer is probed. However, additional techniques are required to complement inherent limitations of STM, such as its inability to look into buried layers and problems concerning the identification and distinction of atomic species. In this paper, we will introduce a new technique to study intermixing and interdiffusion effects in heteroepitaxial growth: Auger-electron spectroscopy (AES) induced by grazingly incident protons in combination with conventional electron-induced AES.[4] We will show that the different sampling depths in proton- and electron-induced AES allow one to obtain layer-dependent concentration profiles of condensate and substrate atoms within a few layers beneath the surface with (near) monolayer resolution.

We have studied the system Cr on Fe(100), which has interesting magnetic properties. It is the basic building block of Fe/Cr/Fe sandwiches and superlattices, which have served as a model system to study phenomena of exchange coupling between ferromagnetic layers separated by nonferromagnetic spacer layers.[5] Whereas for Cr coverages larger than 3 ML the surface magnetization shows a clear layer-by-layer antiferromagnetic stacking,[6] important and unexplained anomalies in the magnetic properties appear at lower coverages. Recent Auger-electron forward scattering[7] and STM studies[3] have revealed a potential structural cause of these anomalies: the authors find that for growth at 570 K no atomically abrupt interface is formed, but intermixing occurs for coverages below 1 ML. For coverages beyond 2 ML the film surface seems to be predominantly Cr.

Our experimental procedure is based on recording Auger signals from Fe and Cr during exposure of the Fe(100) surface to a constant flux of Cr vapor. The Auger electrons are induced either by 4-keV electrons at oblique incidence or by 25-keV protons under grazing incidence. In case of electron-induced AES, the sampling depth is essentially determined by the escape depth of the Auger electrons and amounts to about two layers for the low-energy Auger line of Fe at 47 eV and six layers for the high-energy Auger line at 703 eV (see below). The situation is different for proton-induced AES: Grazingly incident protons cannot overcome the collective repulsive interaction potentials with surface atoms, but are specularly reflected (''planar surface channeling''). Creation of Auger electrons via core-hole excitation is thus confined to atoms in the topmost surface layer, i.e., the sampling depth amounts to one layer, irrespective of the Auger-

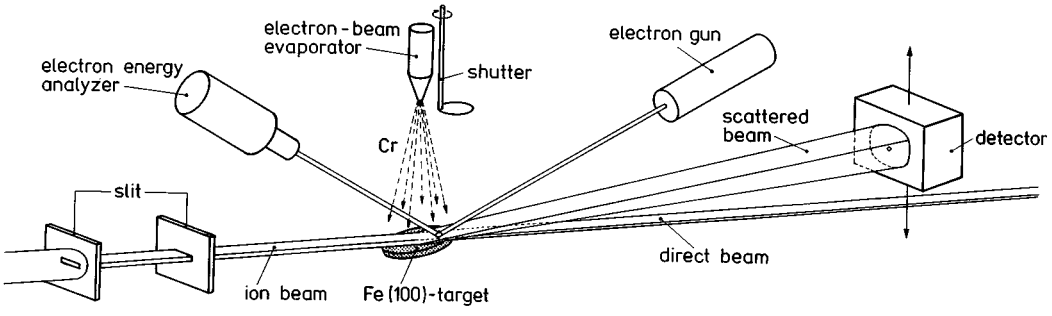

FIG. 1. Sketch of the experimental setup.

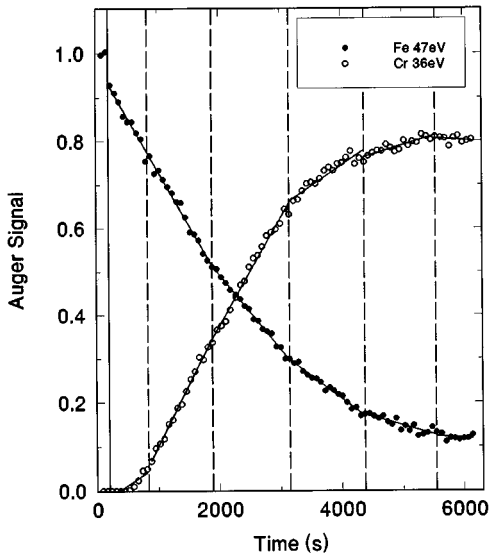

FIG. 2. Electron-induced Fe 47-eV Auger signal (solid circles) and Cr 36-eV Auger signal (open circles) during growth of about 5 ML Cr on Fe(100) at 570 K. The solid lines are the results of a piecewise least-squares straight-line fit to the data. The vertical solid line indicates the opening of the shutter. The vertical dashed lines indicate the completion of atomic layers as obtained from maxima in the intensity of specularly reflected projectiles and breakpoints in the Fe Auger signal. The Auger signals have been normalized to the Fe signal for the clean surface. [The initial drop of the Fe signal reflects the short supersaturation at the beginning of growth to artificially enhance the density of nuclei (Refs. 13, 14, and 9).]

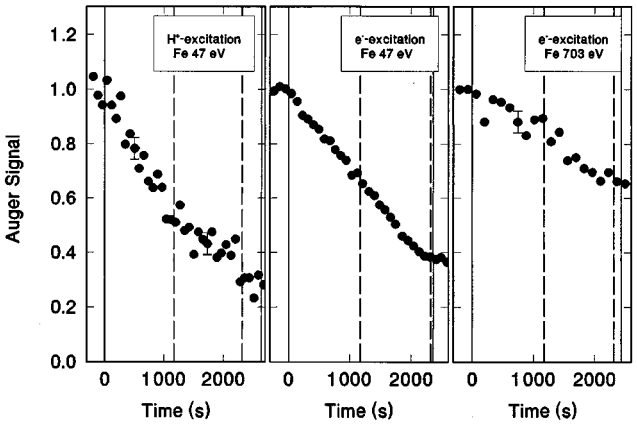

FIG. 3. Proton-induced Fe 47-eV Auger signal (left panel), electron-induced Fe 47-eV Auger signal (central panel), and electron-induced Fe 703-eV Auger signal (right panel) during growth of about 2 ML Cr on Fe(100) at 570 K. The left and right vertical solid lines indicate the opening and closing of the shutter, respectively. The vertical dashed lines indicate the growth of 1 and 2 ML Cr, respectively. All signals are normalized to the data for the clean surface.

electron escape depth. This has been proved for layer-by-layer growth of Ag on Cu(111): When the Cu surface is covered by only 1 ML Ag, the proton-induced Cu Auger signal is reduced to merely 2% from the clean-surface signal.[4]

Simultaneously with Auger electrons, we measured the intensity of specularly reflected protons. In case of a layer-by-layer growth, the intensity depends on the coverage in an oscillatory way,[8,9] similar to the well-known oscillations in reflection high-energy electron diffraction (RHEED). This enables one to count the number of grown layers and precisely determine the completion of a new layer.

Essential components of the experimental setup are sketched in Fig. 1. The proton beam is incident upon the Fe(100) surface at a grazing angle $\Phi_{in}=1.4°$ along a high-index surface lattice direction with a maximum angular divergence of $\pm 0.05°$ and a typical current density of 50 nA/mm^2. The incidence angle of the electron beam is $\Phi_{in}=33°$, its current density is typically 1 μA/mm^2. Those electrons which are emitted by electron or proton impact in a direction oblique to the target surface (75°) are energy analyzed by a 150° spherical sector analyzer (100 mm mean radius) with a transfer lens system (CLAM2). The electron-energy spectra were recorded using pulse counting detection with a constant relative energy resolution $\Delta E/E$ of

TABLE I. Relative Fe Auger signals after growth of 1 ML and 2 ML Cr on Fe(100) at 570 K and layer-dependent Cr concentration derived from it.

	1 ML Cr		
	H^+, 47 eV	e^-, 47 eV	e^-, 703 eV
Fe signal (experiment)	0.53±0.02	0.70±0.02	0.86±0.01
Fe signal (calculation)	0.550	0.706	0.858
	top layer	second layer	third layer
Cr concentration	0.45±0.03 ML	0.55±0.05 ML	0.00±0.10 ML
	2 ML Cr		
	H^+, 47 eV	e^-, 47 eV	e^-, 703 eV
Fe signal (experiment)	0.33±0.03	0.45±0.03	0.70±0.02
Fe signal (calculation)	0.300	0.464	0.728
	top layer	second layer	third layer
Cr concentration	0.70±0.05 ML	1.00±0.15 ML	0.30±0.25 ML

about 0.5% for electron excitation and 2% for proton excitation. The intensity of reflected protons is monitored by means of a channeltron detector, which is positioned into the maximum of the angular distribution of the scattered beam ($\Phi_{out} \approx \Phi_{in}$).

The (100) face of an Fe single crystal was prepared *in situ* by frequent cycles of grazing sputtering with 25-keV Ar^+ ions and subsequent annealing at 860 K. During sputtering the target is rotated around its surface normal to achieve a uniform removal of material. Preparation of the surface was finished when the angular distribution of scattered protons was narrow, Low-energy electron diffraction showed a sharp (1×1) diffraction pattern, and no more impurities could be detected by electron-induced AES.

High-purity Cr is deposited by crucible-free electron beam evaporation. Precise adjustment and continuous control of the flux are allowed by a shutter and an integrated flux monitor. A quartz microbalance can be driven into the vapor beam to calibrate and occasionally check the flux monitor. Growth rates were typically 10^{-3} ML/s. The substrate temperature during evaporation is held constant at 570 ± 5 K, which was measured by a thermocouple. The pressure in the UHV chamber is 3×10^{-11} mbar and below 10^{-10} mbar during Cr evaporation.

In our experiment, we recorded the Fe Auger spectra at 47 and 703 eV in the case of electron excitation and 47 eV in the case of proton excitation. The Auger signal is evaluated from the peak-to-peak height in the numerically differentiated $N(E)$ spectra. We tentatively extracted the Auger signal from the original $N(E)$ spectra by proper background subtraction and integration. Comparison of the two methods for the same data sets did not show significant differences, i.e., changes of Auger line shapes with coverage are negligible and do not affect the peak-to-peak heights. The Auger spectrum of Cr resembles the Fe spectrum. Proper Auger lines are at 36 and 529 eV. Evaluation of the 36-eV line, however, turned out to be ambiguous for small coverages ($\lesssim$0.5 ML) due to a change in background slope, which leads to an underestimation of the signal from the peak-to-peak height.

In Fig. 2 we show the electron-induced Auger signal versus time plots for the Fe 47-eV Auger line (solid circles) and the Cr 36-eV line (open circles) during growth. The Auger signals follow a series of linear variations with break points, where the slope changes abruptly. The break-point positions for Fe and Cr fairly coincide and correspond to maxima in the intensity of specularly reflected projectiles (vertical dashed lines in Fig. 2). The piece-wise linear variation shows that growth proceeds in a layer-by-layer mode, in agreement with recent RHEED,[6] STM,[10] and ion-scattering studies.[9] We note that the first break point for the Fe signal is missing, which indicates deviations from ideal layer-by-layer growth.

From Auger signal versus time plots comprising several ML, the escape depth λ of the Auger electrons can be inferred. Assuming that the overlayer consists predominantly of Cr for film thicknesses larger than 2 ML and that the escape probability decreases exponentially with film thickness, we get $\lambda=2.2\pm0.1$ ML. A corresponding analysis for the high-energy Auger line yields $\lambda=5.9\pm0.4$ ML. These values closely match the values derived from theoretical inelastic mean free paths,[11] when the experimental geometry

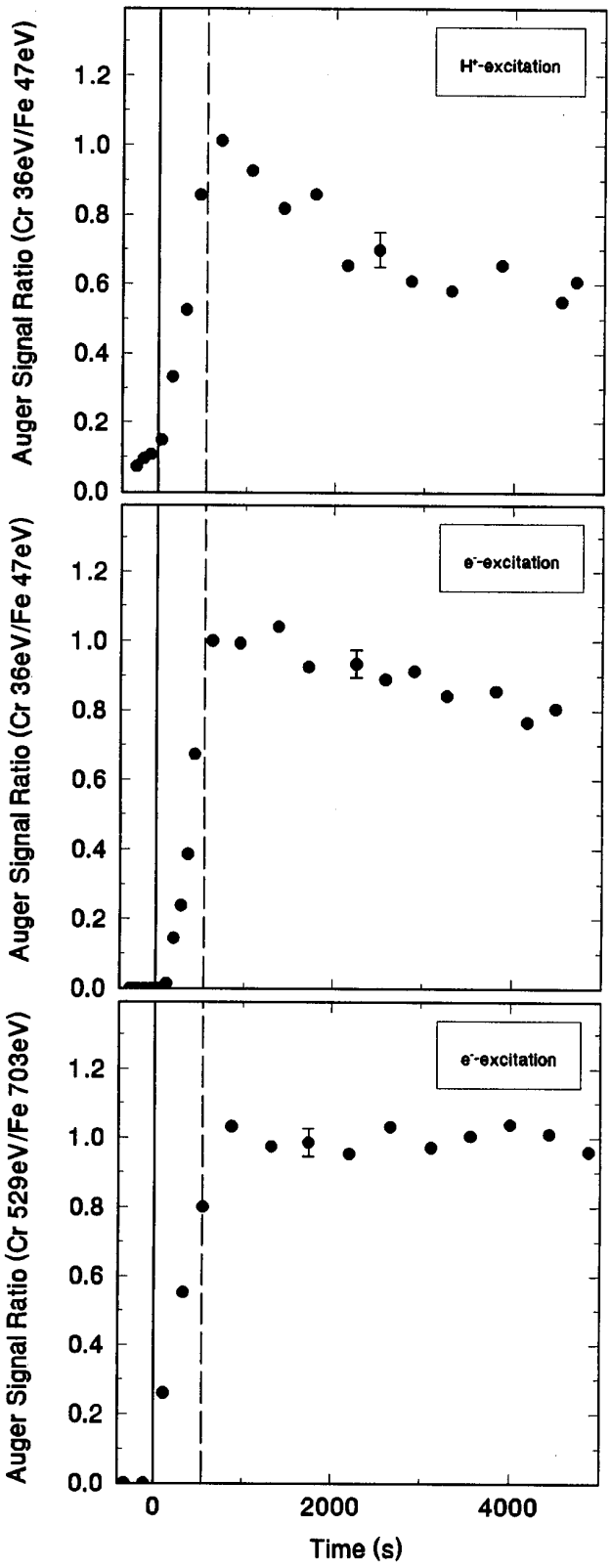

FIG. 4. Proton-induced Cr 36-eV/Fe 47-eV Auger signal ratio (top panel), electron-induced Cr 36-eV/Fe 47-eV Auger signal ratio (central panel), and electron-induced Cr 529-eV/Fe 703-eV Auger signal ratio (bottom panel) as a function of time after growth of 1 ML Cr on Fe(100) at 570 K. The vertical solid line indicates the opening of the shutter. The vertical dashed line indicates the growth of 1 ML Cr and closing of the shutter. All signal ratios are normalized to the data for 1 ML Cr/Fe(100).

and the (weak) attenuation of the primary beam are taken into account[12] ($\lambda = 2.7$ and 6.1 ML, respectively).

In Fig. 3, the decrease of the Fe Auger signals during growth of 2 ML Cr is shown. For proton-excitation, the 47-eV Auger signal (left panel) does not drop to zero, as is expected for a pure Cr overlayer. This shows that the growth layer consists of a mixture of Fe and Cr atoms. The decrease of the electron-excited Auger signal at 47 eV (central panel) and, especially, at 703 eV (right panel) is less, which points to a concentration gradient of Cr within the first few layers. From the relative Auger signals at 1 and 2 ML, the corresponding layer-dependent Cr concentration profiles can be derived. We therefore calculated the decrease of the Auger signals under continuous variation of the Cr concentration within five layers beneath the surface. The results of a least-squares fit to the experimental data are shown in Table I. For 1 ML, the grown adlayer consists of 45% Cr and 55% Fe atoms. For the second layer, the ratio is just reversed. The third and deeper layers solely consist of Fe atoms. We note that this result does not change when the escape depths are varied within $\pm 2\sigma$, or when the constraint concerning the amount of Cr deposited is omitted.

Our results show that about half of the deposited Cr atoms have undergone place exchange with Fe substrate atoms. This interlayer transport process competes with lateral migration of Cr atoms, leading to nucleation and growth of mixed adlayer islands. With further Cr deposition, this scenario continues. Now, however, the top substrate layer is already a mixture of Cr and Fe atoms and exchange processes between Cr adatoms and Fe substrate atoms should be less probable, leading to a larger Cr concentration in the adlayer for a coverage of 2 ML (70%) compared to the adlayer concentration at 1 ML (45%) (see Table I). Nevertheless, 30% of the Cr atoms deposited did exchange places with underlying Fe atoms, which means that the second layer should now predominantly consist of Cr, in agreement with our observation (100%). The fact that no Cr atoms are found from the third layer for 1 ML coverage and, consistently, from the fourth layer for 2 ML, indicates that place exchange processes within buried layers are less probable.

In order to test the stability of grown films, we measured the Auger signals after evaporation of 1 ML as function of time at 570 K (Fig. 4). To compensate for signal fluctuations due to long-term drifts of primary beam current and incidence angle of the protons, we simultaneously measured both the Cr and Fe Auger signals and evaluate the Cr/Fe signal ratios. For proton excitation, this ratio in fact decreases with time to 0.6 from the initial value after about 3000 s (Fig. 4, top panel). When we consider that the initial concentration of Cr atoms in the top layer is 45%, a crude approximation yields a further reduction of the Cr concentration to about 35%. This result is corroborated by the ratio between the electron-induced low-energy Auger signals (Fig. 4, central panel), which decreases only to about 0.8 from the initial value. Because the sampling depth is about two layers, this is in qualitative accordance with our finding that Cr atoms migrate into the second layer but not deeper. The ratio between the high-energy Auger signals, where the sampling depth is six layers, should thus stay constant, as actually observed (Fig. 4, bottom panel).

In summary, we have shown that although growth of Cr on Fe(100) proceeds in a layer-by-layer mode at 570 K, the interface formed is not atomically abrupt. Exploiting the different sampling depths in proton- and electron-induced AES, we could determine the layer-dependent concentration profile of Cr and Fe within a few layers beneath the film surface. We find that intermixing is essentially confined to two or three layers and proceeds within a time of roughly 10^3 s. The results thus essentially confirm recent findings of Venus and Heinrich,[7] who observed by Auger-electron forward scattering that about half of the Cr is below the surface.

We would like to thank R. J. Celotta and R. J. Behm for communicating information prior to publication. The assistance of R.-A. Noack and H. W. Ortjohann (Münster) in the preparation of the experiments is gratefully acknowledged. This work was supported by the Deutsche Forschungsgemeinschaft (Sonderforschungsbereich 290).

[1] E. Bauer, Appl. Surf. Sci. **11/12**, 479 (1982); E. Bauer and J. H. van der Merwe, Phys. Rev. B **33**, 3657 (1986).

[2] See, e.g., S.-L. Chang, J.-M. Wen, P. A. Thiel, S. Günther, J. A. Meyer, and R. J. Behm, Phys. Rev. B (to be published) and references therein.

[3] A. Davies, J. A. Stroscio, D. T. Pierce, and R. J. Celotta, Phys. Rev. Lett. **76**, 4175 (1996).

[4] R. Pfandzelter and J. Landskron, Phys. Rev. Lett. **70**, 1279 (1993).

[5] See D. T. Pierce, J. Unguris, and R. J. Celotta, in *Ultrathin Magnetic Structures II*, edited by B. Heinrich and J. A. C. Bland (Springer, Berlin, 1994), p. 117, and references therein.

[6] J. Unguris, R. J. Celotta, and D. T. Pierce, Phys. Rev. Lett. **69**, 1125 (1992); D. T. Pierce, R. J. Celotta, and J. Unguris, J. Appl. Phys. **73**, 6201 (1993).

[7] D. Venus and B. Heinrich, Phys. Rev. B **53**, R1733 (1996).

[8] Y. Fujii, K. Narumi, K. Kimura, M. Mannami, T. Hashimoto, K. Ogawa, F. Ohtani, T. Yoshida, and M. Asari, Appl. Phys. Lett. **63**, 2070 (1993).

[9] T. Igel, R. Pfandzelter, and H. Winter, Europhys. Lett. (to be published).

[10] D. T. Pierce, J. A. Stroscio, J. Unguris, and R. J. Celotta, Phys. Rev. B **49**, 14 564 (1994).

[11] S. Tanuma, C. J. Powell, and D. R. Penn, Surf. Interface Anal. **17**, 911 (1991).

[12] K. Nishimori, H. Tokutaka, and K. Takashima, Surf. Sci. **100**, 665 (1980).

[13] V. A. Markov, O. P. Pchelyakov, L. V. Sokolov, S. I. Stenin, and S. Stoyanov, Surf. Sci. **250**, 229 (1991).

[14] G. Rosenfeld, R. Servaty, C. Teichert, B. Poelsema, and G. Comsa, Phys. Rev. Lett. **71**, 895 (1993).